High-angle scattering of fast electrons from crystals containing heavy elements: Simulation and experiment

James M. LeBeau,[1,*] Scott D. Findlay,[2] Xiqu Wang,[3] Allan J. Jacobson,[3] Leslie J. Allen,[4] and Susanne Stemmer[1,†]
[1]*Materials Department, University of California, Santa Barbara, California 93106-5050, USA*
[2]*Institute of Engineering Innovation, School of Engineering, The University of Tokyo, Tokyo 113-8656, Japan*
[3]*Department of Chemistry, University of Houston, Houston, Texas 77204, USA*
[4]*School of Physics, University of Melbourne, Victoria 3010, Australia*
(Received 18 February 2009; published 17 June 2009)

The paper reports on quantitative comparisons of experimental and simulated image intensities in high-angle annular dark-field imaging in scanning transmission electron microscopy of a $PbWO_4$ single crystal. The experimental image intensities are normalized to the incident beam. Provided that the effects of spatial incoherence and multiple thermal diffuse scattering events are taken into account in the simulations, excellent agreement within about 5% is achieved between theory and experiments. The comparisons depend critically on accurate knowledge of the Debye-Waller factors, which were determined by x-ray single-crystal structure refinement, and of the experimental thickness values. The Debye-Waller factors are different for different atomic columns, causing column intensities to not be a simple function of their atomic number. Channeling effects associated with the oxygen columns contribute to intensity variations between the Pb and W columns. The results show that even for single crystals, image simulations are required to correctly interpret the contrast.

DOI: 10.1103/PhysRevB.79.214110 PACS number(s): 68.37.Ma, 61.05.jd, 61.05.jm

I. INTRODUCTION

Atomic resolution high-angle annular dark-field (HAADF) (or *Z*-contrast) imaging in scanning transmission electron microscopy (STEM) is rapidly emerging as one of the most important techniques for the direct determination of interface and defect atomic structures in materials. In addition, because the image contrast in HAADF is highly sensitive to the atomic number (Z), these images can provide information on the type of species in the atomic columns. Two of the present authors (J.M.L. and S.S.) have recently developed a method to place experimental HAADF images on an absolute intensity scale, allowing for direct comparisons with image simulations without any need for scaling.[1] Quantitative comparisons with image simulations of $SrTiO_3$ crystals showed excellent agreement,[2] provided that the simulations account for thermal diffuse scattering (TDS) to all orders (i.e., all multiple thermal scattering event sequences) and spatial incoherence. The excellent match is in sharp contrast to conventional high-resolution transmission electron microscopy (HRTEM), based on parallel imaging with electrons elastically scattered to low angles, where a large contrast mismatch known as the "Stobbs factor" is observed.[3–6]

The goal of the present study was to investigate if the excellent agreement between experiment and simulation in quantitative HAADF also applies to crystals containing heavier elements than those in $SrTiO_3$. In particular, in a previous study of HAADF images of an epitaxial $PbTiO_3$ thin film, a contrast mismatch was observed,[7,8] which could not be accounted for by the multiple scattering and spatial incoherence alone. One can envisage both theoretical and experimental reasons for the mismatch. For instance, on the theoretical side, Anstis[9] has suggested that the phase grating (or Molière) approximation on which the standard simulations are founded breaks down for heavy elements at large scattering angles. On the experimental side, thin-film materials are subject to mismatch strain and nonstoichiometry, which are typically not included in simulations. Analysis of the possible causes of the discrepancy from that data set was further hindered because the experimental images were not acquired on an absolute scale. To avoid strain and nonstoichiometry, the present study uses a single crystal of lead tungstate ($PbWO_4$), which contains two cations with relatively large Z ($Z_{Pb}=82$ and $Z_W=74$). By establishing that excellent quantitative agreement between experiment and simulation can be achieved for heavy elements in a well-characterized specimen, the discrepancies noted previously could become a source of further information about the material.

II. EXPERIMENTAL

A single crystal of $PbWO_4$ with the tetragonal scheelite structure[10] was obtained from MTI Corporation (Richmond, CA). The crystal was prepared for electron microscopy along [100] by wedge polishing followed by argon-ion milling (Fischione model 1010). To remove amorphous surface layers, the sample was chemically etched in a 0.75 N NaOH solution for approximately 2 min. The sample was then returned to the ion mill for a short period (<3 min). To avoid charging, the sample was coated with an approximately 0.9-nm-thick carbon layer. An FEI Titan 80–300 kV S/TEM operating at 300 kV was used for HAADF-STEM ($C_s \sim 1.2$ mm). The STEM imaging conditions were set as follows: extraction voltage of 4400 kV, spot size of 10, gun lens of 6, and a convergence semiangle of 9.4 mrad. The focus (~ 51 nm underfocus) was determined using the maximum intensity criterion in both experiments and Bloch wave simulations, as described previously.[2,11] A Gatan Enfina spectrometer was used for electron energy-loss spectroscopy (EELS).

The thickness at each image location was measured by using both the EELS log-ratio method[12] and zone-axis convergent beam electron-diffraction (CBED) patterns that were compared with simulations. For EELS, the inelastic mean-free path was estimated to be 105 nm from an empirical estimate given by Egerton.[12] Position-averaged CBED (PACBED) patterns were acquired with a Gatan Ultrascan 1000 charge-coupled device camera while rapidly scanning the probe across the area of the image. This allowed measurement of the thickness directly after the acquisition of the HAADF image with no need to change the optical parameters of the microscope. The thickness for each experimental PACBED pattern was determined by comparisons with patterns calculated with Bloch wave simulations. Fine details in the PACBED patterns change rapidly with thickness, allowing for a thickness determination accuracy of $\pm 2-4$ nm by comparison with simulations.[13] For very thin regions (<30 nm), the PACBED patterns could be matched to within ± 1 nm.

The HAADF signal was measured with a Fischione model 3000 HAADF detector set to an inner detector semiangle of 65 ± 1 mrad and an outer semiangle of approximately 350 mrad. The incident-beam intensity and image intensities were acquired with a National Instruments dynamic signal analyzer (model 4474) connected to the detector preamplifier, as described previously.[1] Because the HAADF detector has a nonuniform detection efficiency, the effective incident-beam intensity was determined by averaging the detector output from 65–130 mrad.[1] The images were acquired with a dwell time of 49.07 μs and a frame size of 512×512. To account for noise within the images, the maximum image signal was defined as the intensity at which 1.5% of the total number of image pixels (~ 3700 pixels) fell below the absolute maximum image signal. The 1.5% value was chosen based on the noise level of the images and so that the maximum intensities at the column positions were within this range. The minimum ("background") signal was defined as the largest intensity for which 1.5% of all image pixel values were above the absolute minimum image signal.

The multislice frozen phonon approach[2,11,14] was used for simulating the theoretical image intensities of $PbWO_4$ because it correctly accounts for multiple thermal diffuse scattering events.[2,14] The outer detector semiangle for the calculations was 240 mrad, based on the sampling bandwidth limit. Such simulations are inherently carried out for a point source but a finite effective source size, or spatial incoherence, can be readily included in postprocessing.[15] To check whether approximations made in the standard simulation theory break down for the heavy elements in this specimen,[9] we have compared the standard frozen phonon calculations with calculations which make corrections for higher-order Laue zones[16] and with multislice calculations using a very finely sliced three-dimensional potential.[17] In both cases, the more elaborate calculations were in good agreement with the standard simulations. We also checked the performance against standard tabulations[18] of differential scattering cross sections for scattering of Pb at 80 keV calculated using a partial-wave expansion and found agreement. This agreement is expected to be even better at 300 keV. That these higher order methods do not significantly change the results suggests that the standard approach should still be adequate for this specimen.

TABLE I. Fractional atom coordinates and Debye-Waller factors (B) in $PbWO_4$ in space-group $P4$ with $a=0.7725$ nm and $c=1.2048$ nm.

Atom	x	y	z	B (nm^2)
Pb (1)	0.7487	0.2509	0.2494	0.0165
Pb (2)	0.5000	0.0000	0.5000	0.0134
Pb (3)	0.5000	0.5000	0.0000	0.0141
Pb (4)	0.0000	0.0000	0.0000	0.0134
W (1)	0.2491	0.2485	0.2505	0.0123
W (2)	0.5000	0.0000	−0.0003	0.0130
W (3)	0.5000	0.5000	0.5000	0.0121
W (4)	0.0000	0.0000	0.5000	0.0140
O (1)	0.0460	0.1830	0.5800	0.0154
O (2)	0.6870	0.4510	0.4190	0.0154
O (3)	0.0620	0.2930	0.3310	0.0154
O (4)	0.2030	0.0640	0.1670	0.0154
O (5)	0.2980	0.4450	0.1660	0.0154
O (6)	0.3150	0.0430	−0.0820	0.0154
O (7)	0.4330	0.2020	0.3320	0.0154
O (8)	0.5440	0.1850	0.0820	0.0154

The intensities of the atomic columns in HAADF images are sensitive to atomic vibrations;[19] thus, atom displacements in the frozen phonon model require accurate values of the Debye-Waller factor for each atom in the $PbWO_4$ structure. The Debye-Waller factors were determined by x-ray single-crystal structure refinements. For the structure refinement, a Siemens SMART platform diffractometer outfitted with an Apex II area detector and monochromatized Mo K_α radiation was used to measure a crystal (approximate dimensions $0.25 \times 0.25 \times 0.03$ mm^3) at room temperature. The structure was refined using the BRUKER APEX II program package.

III. RESULTS AND DISCUSSION

Similar to reports in the literature[20] x-ray diffraction showed a superstructure that was inconsistent with the $I4_1/a$ space group of the ideal scheelite structure. The structure was thus refined in the space-group $P4$ with a larger unit cell (with the lattice parameter a multiplied by a factor of $\sqrt{2}$) that was consistent with the superstructure and which had previously been suggested for a Pb-deficient phase ($Pb_{7.5}W_8O_{32}$) from neutron-diffraction experiments.[20] The Debye-Waller factors for all oxygen atoms within the structure were constrained to be equal but free to vary during refinement. The Debye-Waller factors[21] for Pb and W were found to range between 0.0134–0.0165, and 0.012–0.014 nm^2, respectively, depending on their position within the unit cell (see Table I). The Debye-Waller factor for the oxygen atoms was 0.0154 nm^2. The refinements converged at $R=0.113$ ($R=\Sigma|\Delta F|/\Sigma|F_o|$) for 572 unique reflections with $I>2\sigma(I)$ and $R=0.155$ for all 1722 unique reflec-

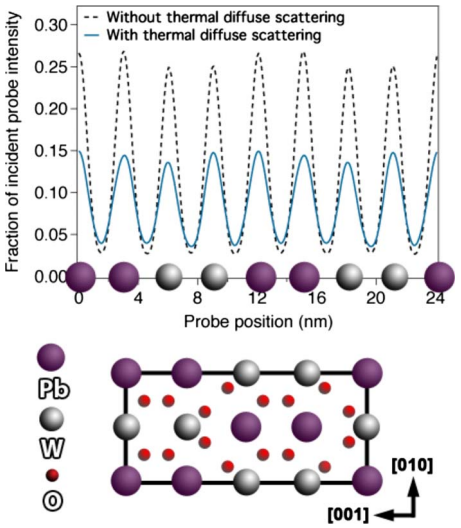

FIG. 1. (Color online) (Top row) Simulated intensity line scan along [001] in a [100] projection for a 17.5-nm-thick $PbWO_4$ sample without thermal scattering (dashed line) and with thermal diffuse scattering (solid line). The effects of spatial incoherence are not taken into account. The line scan is across the Pb and W column pairs. Note that after including thermal diffuse scattering some of the W columns can appear brighter than the Pb columns, opposite to what might be expected from their atomic number. A [100] projection of the scheelite structure is shown in the bottom row.

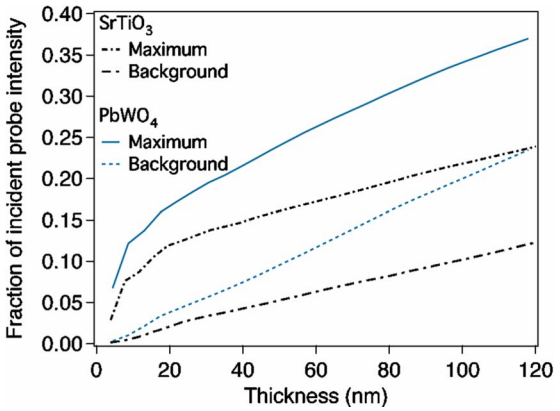

FIG. 2. (Color online) Frozen phonon simulations of the maximum and minimum ("background") image intensities for $SrTiO_3$ and $PbWO_4$ as a function of thickness. The signals increase about twice as fast with thickness for $PbWO_4$ compared to $SrTiO_3$. The effects of spatial incoherence are not taken into account.

tions and 64 variables. The refinement suggested that the Pb positions in this sample were fully occupied, consistent with the composition $PbWO_4$. Thus the superstructure was not due to Pb deficiency. The moderately high R values were probably due to the low accuracy of the superstructure reflections. All crystallographic directions stated in this paper refer to the smaller scheelite unit cell, shown in Fig. 1. In a [100] projection of scheelite $PbWO_4$ (Fig. 1) the Pb and W columns form pairs along [001] and alternate along [010]. The oxygen columns also form pairs but their orientation and spacing alternates.

The experimentally measured Debye-Waller factors were used for the atom displacements in the frozen phonon image simulations accounting for TDS. Figure 1 shows a simulated HAADF intensity line scan along [001] across pairs of Pb and W columns with and without TDS. The term "with TDS" refers to a frozen phonon calculation averaged over several configurations of the atoms (enough to obtain a reasonable convergence). By "without TDS" we mean a simulation in the frozen phonon model using a single configuration with no displacements of the atoms. With TDS, the overall intensity scattered onto the HAADF detector decreases and the contrast is reduced by 19%. Both are caused by a significant decrease in the atomic column intensities due to thermal vibrations. This is different from prior simulation results for Si, where accounting for TDS resulted in no modification of the contrast.[22] Without TDS, the Pb columns would have appeared brighter than the W columns, as expected because of their larger Z. With TDS, however, the Pb and W columns have almost identical intensities. They alternate slightly in intensity (depending on the thickness) because of the different Debye-Waller factors for each column. Thus, a simple intuitive interpretation of the image contrast based on Z is not possible and image simulations are essential for correct interpretation. Furthermore, the Pb and W columns cannot be distinguished in the experiments.

In addition to correctly accounting for Debye-Waller factors in the simulations, accurate measurements of the thickness are essential for comparisons between theory and experiment. In particular, strongly scattering crystals, such as $PbWO_4$, are much more sensitive to errors in the experimental thickness determination than crystals with smaller Z. To illustrate this point, Fig. 2 compares the thickness dependence of simulated image intensities (background and maximum intensity, without spatial incoherence taken into account) for $SrTiO_3$ and $PbWO_4$. The background signal increases with thickness by about a factor of two faster in $PbWO_4$ than in $SrTiO_3$.

In this study, an estimate of the experimental thickness for each image was first attempted using EELS.[12] The thickness values obtained from EELS, however, exhibited significant scatter, most likely due to nonuniform surface contributions (i.e., carbon surface layers).[2,12] In contrast, the PACBED patterns (see Fig. 3 for an example) yield precise and highly accurate thickness values that are very sensitive to small changes in thickness. Although PACBED relies on comparison with pattern simulations, further validation of its accuracy comes from analyzing image intensities as a function of thickness determined by PACBED. Figure 4 shows a comparison of *mean* HAADF image intensities in simulation and experiments as a function of thickness, which was obtained by PACBED in the experiments. Excellent agreement was obtained across the entire thickness range. It should be noted that the mean image intensity is not influenced by spatial incoherence or instabilities, which results in a redistribution of images intensities,[23] relative to the incident probe, in contrast to the maximum and minimum image signals considered next.

Figure 5 shows a comparison of the experimental and simulated image signals. The maximum atom column intensities differ by a factor of 1.2–1.3 if simulations do not take into account the cumulative effects of a finite source size,

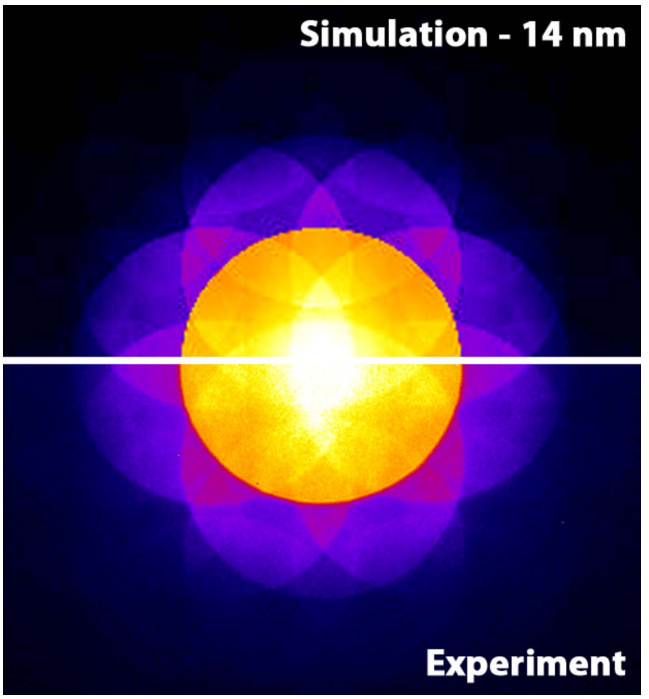

FIG. 3. (Color online) Simulated (top half) and experimental (bottom half) PACBED patterns along [100] for a 14-nm-thick region of $PbWO_4$.

sample vibration, or any other sources contributing to spatial incoherence (dashed lines). A similar mismatch is observed for the background signal. To model the influence of spatial incoherence, the simulated images were convolved with a Gaussian function.[11,15] Figure 5 shows that after convolution with a Gaussian with a 0.115 nm full width at half maximum (FWHM), excellent agreement between experiments and simulations is obtained (see Appendix for a discussion of the effective source size). After convolution, the match between experiments and simulations is within about 5% (mean error). It should be noted that if the $PbWO_4$ structure was

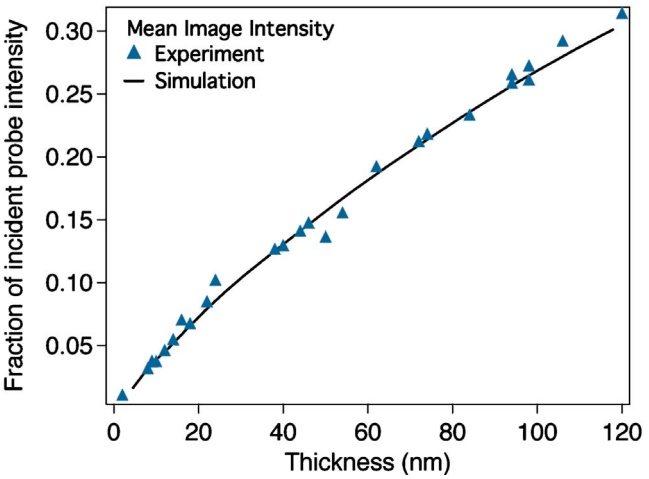

FIG. 4. (Color online) Comparison of the mean image intensity for experimental (symbols) and simulated (line) images as a function of thickness. The experimental thickness was determined from PACBED patterns.

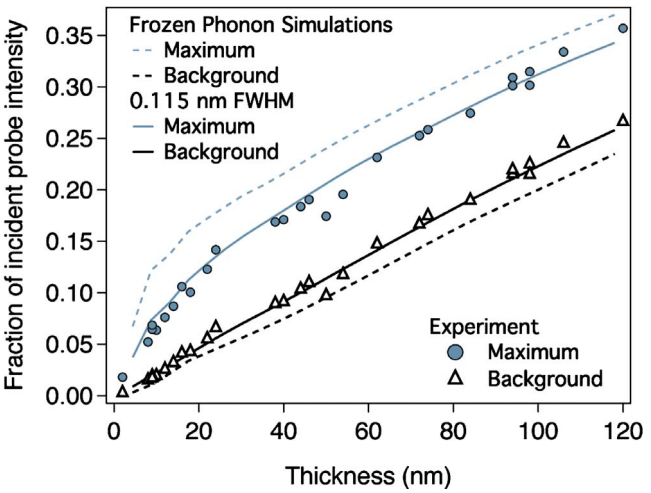

FIG. 5. (Color online) Comparison of experimental (symbols) and simulated (line) image signals as a function of thickness. Both the maximum signal and minimum ("background") signal are shown. The dashed and solid lines represent simulations without and with the effects of spatial incoherence taken into account by convolution with a 0.115 nm FHWM Gaussian, respectively. The difference in signals between experiments and simulations after convolution is less than 5% on average.

refined using the ideal scheelite space group, slightly different Debye-Waller factors were obtained compared to those obtained in the refinement including the superstructure. Using the Debye-Waller factors obtained for the ideal scheelite structure resulted in only a slight increase in the background. The conclusions in this paper concerning the HAADF image intensities are not affected by whether or not the structure was refined in the larger unit cell or the ideal scheelite structure. Figure 6 shows experimental and simulated images for different thicknesses, confirming the excellent agreement for the entire thickness range.

Although the oxygen columns are not directly visible in the images in Fig. 6, their arrangement is intimately connected to the change in background intensity as a function of thickness. In particular, for thicknesses greater than about 40 nm the background exhibits an alternating pattern, being highest in the locations were the oxygen atoms are located furthest from one another in the projected structure but closest to the heavy W columns. The scattering potential of oxygen is too weak to contribute much directly to the HAADF images, or to significantly bind the channeling probe. But the oxygen atoms can have an appreciable effect on the evolving electron intensity distribution. Basically, a probe positioned between an oxygen column pair will spread preferentially in the direction of the oxygen columns. For those column pairs aligned diagonally relative to the conventional unit cell shown in Fig. 1, this serves to transfer electron density toward the strongly channeling W columns. The column pairs aligned along the [001] direction in Fig. 1 do not as effectively transfer electron density to the cation columns. This difference is responsible for the alternating background contrast seen in Fig. 6.

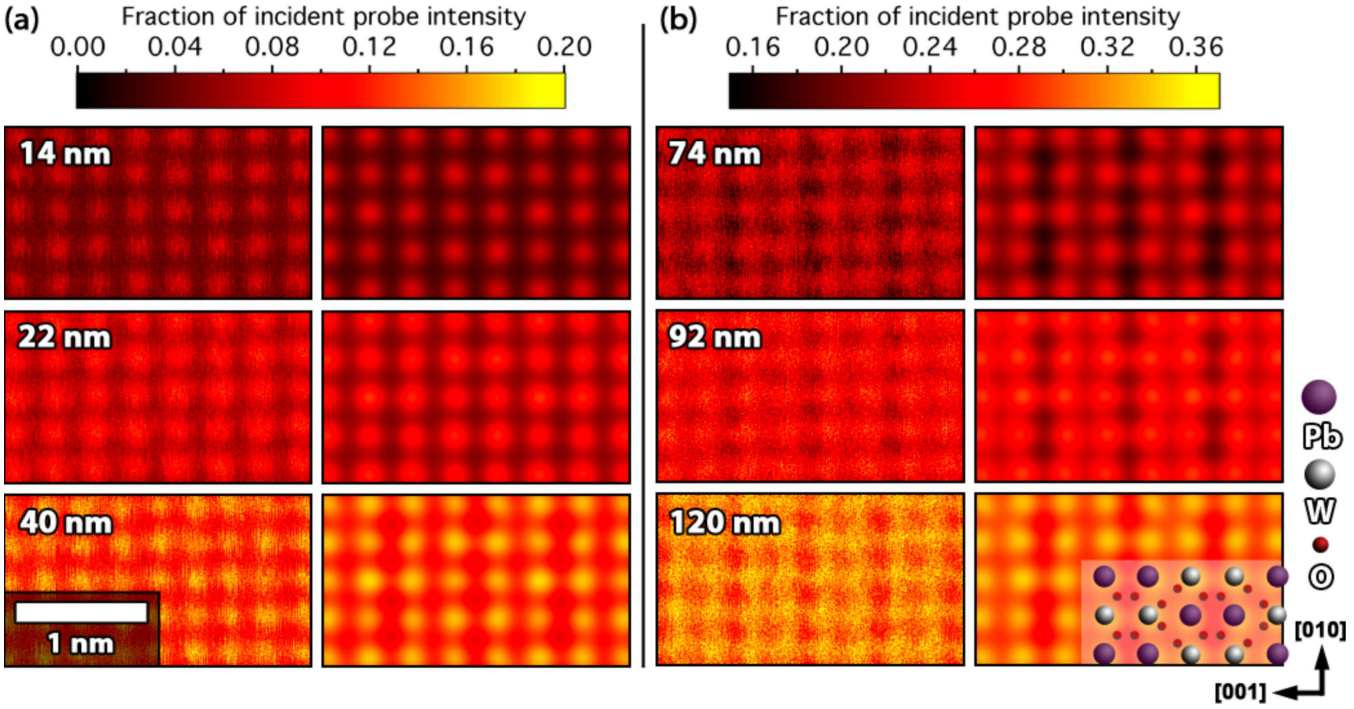

FIG. 6. (Color online) Experimental (left panels) and simulated (right panels) images for different thicknesses (see labels). The simulated images account for finite source size characterized by a 0.115 nm FWHM Gaussian distribution. Note that different intensity scales are used in (a) and (b) for clarity. The uncertainties in the experimental thicknesses are $\pm 2-4$ nm and the simulated thicknesses are within ± 2 nm of the value given in the figure.

IV. CONCLUSIONS

In summary, by placing the experimental image HAADF intensities on an absolute scale, direct comparisons between experimental image intensities and frozen phonon image simulations could be made. Excellent agreement within 5% of the experimentally measured signals was achieved. The results presented here and those previously reported for $SrTiO_3$ (Ref. 2) show that the agreement in HAADF is far better than in conventional HRTEM, where a mismatch corresponding to a factor of two to three is usual.[5,6] Spatial incoherence has to be taken into account in the simulations. This parameter is difficult to measure independently in non-aberration corrected STEM,[24] although the good agreement demonstrated here for a wide range of specimen thicknesses and for different materials supports its determination by comparison with simulation for well-characterized specimens.

The results also point to potential challenges in quantitative HAADF. In particular, comparisons with simulations for crystals with heavy elements are much more sensitive to errors in foil thickness measurements than those for more weakly scattering materials. A second challenge is knowledge of the Debye-Waller factor of each atom. While Debye-Waller factors can be measured for bulk materials, this is not the case at interfaces or near defects. Previous reports of a large contrast mismatch between simulations and experiments of $PbTiO_3$ films may have originated from neglecting TDS in the simulations[7] and/or the unknown magnitude of the Debye-Waller factor in epitaxially strained films.[8] These errors are in addition to any errors in thickness measurement by EELS, which has been shown to be very sensitive to surface effects in some materials, in particular the perovskites.[2] Most importantly, the study has shown that, because of the great sensitivity to thermal vibrations and channeling effects, image simulations are required to fully understand the image contrast, contrary to common perception that HAADF-STEM images are intuitively interpretable in terms of the atomic numbers present. The excellent agreement between simulations and experiments points to the exciting possibility of imaging previously unknown parameters, such as Debye-Waller factors in strained films or around defects.

ACKNOWLEDGMENTS

The authors gratefully acknowledge assistance from Adrian D'Alfonso in checking the scattering cross sections. The research at UCSB was supported by the U.S. National Science Foundation (Grant No. DMR-0804631). J.M.L. also thanks the U.S. Department of Education for support through the GAANN program (Grant No. P200A07044) and the NSF-funded UCSB ICMR (Contract No. DMR-0409848) for a travel grant to Melbourne to work with L.J.A. The work made use of the UCSB MRL Central facilities supported by the MRSEC Program of the National Science Foundation under Award No. DMR 0520415. L.J.A. acknowledges support by the Australian Research Council. S.D.F. is supported by the Japan Society for the Promotion of Science (JSPS). A. J. J. and X. W. acknowledge support from the R. A. Welch Foundation.

APPENDIX: COMMENT ON THE EFFECTIVE SOURCE SIZE

Schottky field emitters are not entirely stable over time because the high extraction electric field causes atom migration at the tip.[25] In an earlier study (~12 months prior to the data acquisition in this study) with the same field-emitter tip, accounting for the effective source size via a convolution of the simulated images with a Gaussian envelope of 0.08 nm resulted in excellent agreement between experiments and simulations of $SrTiO_3$.[2] In contrast, in a more recent investigation of $SrTiO_3$ (approximately the same time as the $PbWO_4$ data were acquired), a convolution with a 0.11–0.12 nm FWHM Gaussian was required to achieve the same excellent agreement, as shown in Fig. 7. Although part of this might be due to the more accurate thickness determination in this study using PACBED, the degradation of the field emitter over time apparently influences the effective source size in STEM. The convolution with a FWHM of 0.12 nm does not reduce the resolution below the experimentally determined value of ~0.136 nm (i.e., the ⟨110⟩ Si dumbbells are still resolved after the convolution). Furthermore, that the same FWHM gives excellent agreement between simulations and experiments for different materials ($SrTiO_3$ and $PbWO_4$) across the entire thickness range shows that it is a good estimate for the spatial incoherence, and possibly to some degree of other effects, such as small misalignments or uncertainties in C_s and defocus. This is in sharp contrast to the effects of the "Stobbs factor" in HRTEM, which was found to vary with experimental conditions such as thickness.[6]

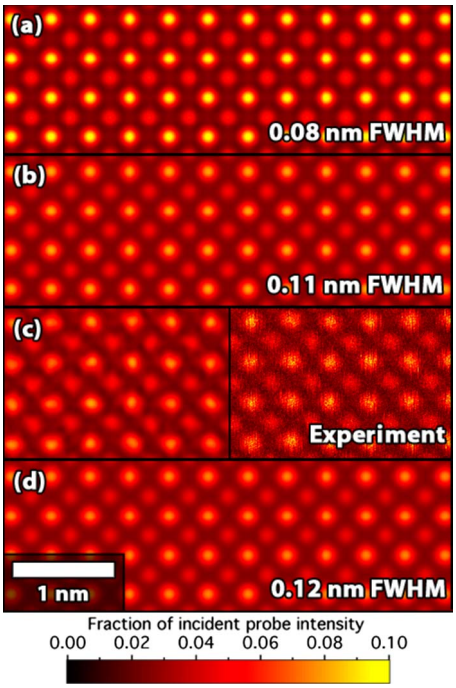

FIG. 7. (Color online) Comparison of simulated 12-nm-thick region of $SrTiO_3$ with different magnitudes of [(a), (b), (d)] the Gaussian FHWM effective source sizes and (c) an experimental image. The right column in (c) shows the original experimental image and the left column after Fourier filtering with a 9.85 nm^{-1} circular aperture. An effective source size with Gaussian FWHM between (b) 0.11 and (d) 0.12 produces the best fit.

*lebeau@mrl.ucsb.edu
†stemmer@mrl.ucsb.edu

[1] J. M. LeBeau and S. Stemmer, Ultramicroscopy **108**, 1653 (2008).
[2] J. M. LeBeau, S. D. Findlay, L. J. Allen, and S. Stemmer, Phys. Rev. Lett. **100**, 206101 (2008).
[3] M. J. Hytch and W. M. Stobbs, Ultramicroscopy **53**, 191 (1994).
[4] A. Howie, Ultramicroscopy **98**, 73 (2004).
[5] C. B. Boothroyd, J. Microsc. **190**, 99 (1998).
[6] K. Du, K. von Hochmeister, and F. Phillipp, Ultramicroscopy **107**, 281 (2007).
[7] D. O. Klenov and S. Stemmer, Ultramicroscopy **106**, 889 (2006).
[8] S. D. Findlay, D. O. Klenov, S. Stemmer, and L. J. Allen, Mater. Sci. Technol. **24**, 660 (2008).
[9] G. R. Anstis, Acta Crystallogr., Sect. A: Found. Crystallogr. **52**, 450 (1996).
[10] A. W. Sleight, Acta Crystallogr., Sect. B: Struct. Crystallogr. Cryst. Chem. **28**, 2899 (1972).
[11] D. O. Klenov, S. D. Findlay, L. J. Allen, and S. Stemmer, Phys. Rev. B **76**, 014111 (2007).
[12] R. F. Egerton, *Electron Energy-Loss Spectroscopy in the Electron Microscope*, 2nd ed. (Plenum, New York, 1996).
[13] J. M. LeBeau, S. D. Findlay, L. J. Allen, and S. Stemmer, (unpublished).
[14] R. F. Loane, P. Xu, and J. Silcox, Acta Crystallogr., Sect. A: Found. Crystallogr. **47**, 267 (1991).
[15] P. D. Nellist and J. M. Rodenburg, Ultramicroscopy **54**, 61 (1994).
[16] J. H. Chen and D. Van Dyck, Ultramicroscopy **70**, 29 (1997).
[17] R. Kilaas, M. A. O'Keefe, and K. M. Krishnan, Ultramicroscopy **21**, 47 (1987).
[18] *International Tables for Crystallography Volume C: Mathematical, Physical and Chemical Tables*, edited by E. Prince (Kluwer, Dordrecht, 2004).
[19] M. Haruta, H. Kurata, H. Komatsu, Y. Shimakawa, and S. Isoda, Ultramicroscopy **109**, 361 (2009).
[20] J. M. Moreau, R. E. Gladyshevskii, P. Galez, J. P. Peigneux, and M. V. Korzhik, J. Alloys Compd. **284**, 104 (1999).
[21] The Debye-Waller factors, also called the temperature B factors, are related to the projected mean-square vibrational amplitude $\langle u^2 \rangle$ via $B = 8\pi^2 \langle u^2 \rangle$.
[22] S. Hillyard and J. Silcox, Ultramicroscopy **58**, 6 (1995).
[23] V. Grillo, E. Carlino, and F. Glas, Phys. Rev. B **77**, 054103 (2008).
[24] C. Dwyer, R. Erni, and J. Etheridge, Appl. Phys. Lett. **93**, 021115 (2008).
[25] L. W. Swanson and G. A. Schwind, in *Handbook of Charged Particle Optics*, edited by J. Orloff (CRC, Boca Raton, 1997).